1-10-2023

Dry eye disease in mice activates adaptive corneal epithelial regeneration distinct from constitutive renewal in homeostasis

Joseph B Lin
Washington University School of Medicine in St. Louis

Xiaolei Shen
Washington University School of Medicine in St. Louis

Charles W Pfeifer
Washington University School of Medicine in St. Louis

Fion Shiau
Washington University School of Medicine in St. Louis

Andrea Santeford
Washington University School of Medicine in St. Louis

See next page for additional authors

PNAS RESEARCH ARTICLE | DEVELOPMENTAL BIOLOGY

Dry eye disease in mice activates adaptive corneal epithelial regeneration distinct from constitutive renewal in homeostasis

Joseph B. Lin[a,b], Xiaolei Shen[c,d], Charles W. Pfeifer[a,b], Fion Shiau[a], Andrea Santeford[a], Philip A. Ruzycki[a], Brian S. Clark[a,e,f], Qin Liu[a,c,d], Andrew J. W. Huang[a], and Rajendra S. Apte[a,e,f,g,1]

Edited by Balamurali K. Ambati, Knight's Campus for Accelerating Scientific Impact, University of Oregon, OR; received March 10, 2022; accepted November 28, 2022 by Editorial Board Member Jeremy Nathans

Many epithelial compartments undergo constitutive renewal in homeostasis but activate unique regenerative responses following injury. The clear corneal epithelium is crucial for vision and is renewed from limbal stem cells (LSCs). Using single-cell RNA sequencing, we profiled the mouse corneal epithelium in homeostasis, aging, diabetes, and dry eye disease (DED), where tear deficiency predisposes the cornea to recurrent injury. In homeostasis, we capture the transcriptional states that accomplish continuous tissue turnover. We leverage our dataset to identify candidate genes and gene networks that characterize key stages across homeostatic renewal, including markers for LSCs. In aging and diabetes, there were only mild changes with <15 dysregulated genes. The constitutive cell types that accomplish homeostatic renewal were conserved in DED but were associated with activation of cell states that comprise "adaptive regeneration." We provide global markers that distinguish cell types in homeostatic renewal vs. adaptive regeneration and markers that specifically define DED-elicited proliferating and differentiating cell types. We validate that expression of SPARC, a marker of adaptive regeneration, is also induced in corneal epithelial wound healing and accelerates wound closure in a corneal epithelial cell scratch assay. Finally, we propose a classification system for LSC markers based on their expression fidelity in homeostasis and disease. This transcriptional dissection uncovers the dramatically altered transcriptional landscape of the corneal epithelium in DED, providing a framework and atlas for future study of these ocular surface stem cells in health and disease.

stem cell | cornea | limbal | epithelium | dry eye

Significance

We resolve cell type-specific transcriptional signatures of corneal epithelial differentiation in health, injury, and disease; identify unique genes and gene networks that may be amenable to therapy for the treatment of ocular surface diseases; and create a framework for future studies of corneal limbal stem cells and other stem cell compartments.

The transparent cornea is the protective anterior surface of the eye that provides an entry point for and initial focus of photons onto the neurosensory retina. The epithelial layer on the corneal surface is constantly renewed by a population of epithelial stem cells that resides in the basal layers of the limbus at the peripheral rim of the cornea that separates it from the surrounding conjunctiva (Fig. 1*A*) (1). The importance of this limbal stem cell (LSC) compartment is highlighted by cases of LSC deficiency resulting from trauma or congenital defects, in which case the corneal epithelium exhibits reduced regeneration that can lead to progressive vision loss (2). Additionally, when LSCs are dysfunctional or deficient, the adjacent conjunctiva may invade the cornea causing corneal vascularization and opacification (i.e., conjunctivalization), resulting in blindness (2).

Despite its unique importance in maintaining vision, the LSC lineage remains poorly characterized. The canonical model of LSC differentiation proposed nearly four decades ago postulates that LSCs give rise to transit amplifying cells (TACs) that extend centripetally toward the central cornea along the basement membrane as they proliferate (Fig. 1*A*) (3, 4). Differentiating cells exit the cell cycle and migrate apically through the stratified corneal epithelium, which includes layers of suprabasal wing cells and the most superficial squamous cells. Recently, studies have demonstrated that there may be another noncanonical pathway of differentiation that gives rise to differentiated cells that extend circumferentially around the limbus (5–7).

In this work, we utilized single-cell RNA sequencing (scRNAseq) to uncover the transcriptional signatures of LSCs and their differentiation in health and disease. In homeostasis, we resolve at the single-cell level all of the cell types that enable constitutive renewal of the corneal epithelium. We identify potential genes and gene networks delineating key stages of differentiation in resting turnover. In models of diabetes and aging, these constitutive cell types appear to be largely unchanged at the transcriptional level. We also examined a murine model of dry eye disease (DED), a condition that affects tens of millions of individuals around the world (8). In DED, an inadequate tear film leads to recurrent injury to the ocular surface. We uncovered that constitutive cell types are maintained in aqueous tear deficiency but observe activation of a previously undescribed disease-state transcriptional program. This DED-induced response likely reflects activation of repair programs following epithelial insults, such as may arise from desiccative stress. We term this "adaptive regeneration." We delineate the unique transcriptional signatures of constitutive tissue turnover and adaptive regeneration in DED. One marker of adaptive regeneration is SPARC, which we validate in corneal epithelial wound healing and identify several SPARC target genes. The scRNAseq dataset of the enclosed work is a significant advance in our understanding of understudied but important ocular

Author affiliations: [a]John F. Hardesty, MD Department of Ophthalmology & Visual Sciences, Washington University School of Medicine, St. Louis, MO 63110; [b]Division of Biology and Biomedical Sciences Neurosciences Graduate Program, Washington University School of Medicine, St. Louis, MO 63110; [c]Center for the Study of Itch and Sensory Disorders, Washington University School of Medicine, St. Louis, MO 63110; [d]Department of Anesthesiology, Washington University School of Medicine, St. Louis, MO 63110; [e]Department of Developmental Biology, Washington University School of Medicine, St. Louis, MO 63110; [f]Center of Regenerative Medicine, Washington University School of Medicine, St. Louis, MO 63110; and [g]Department of Medicine, Washington University School of Medicine, St. Louis, MO 63110

Author contributions: J.B.L., X.S., P.A.R., Q.L., A.J.W.H., and R.S.A. designed research; J.B.L., X.S., C.W.P., A.S., and A.J.W.H. performed research; J.B.L., F.S., P.A.R., B.S.C., A.J.W.H., and R.S.A. analyzed data; and J.B.L. wrote the paper.

The authors declare no competing interest.

This article is a PNAS Direct Submission. B.K.A. is a guest editor invited by the Editorial Board.

[1]To whom correspondence may be addressed. Email: apte@wustl.edu.

This article contains supporting information online at https://www.pnas.org/lookup/suppl/doi:10.1073/pnas.2204134120/-/DCSupplemental.

Published January 3, 2023.

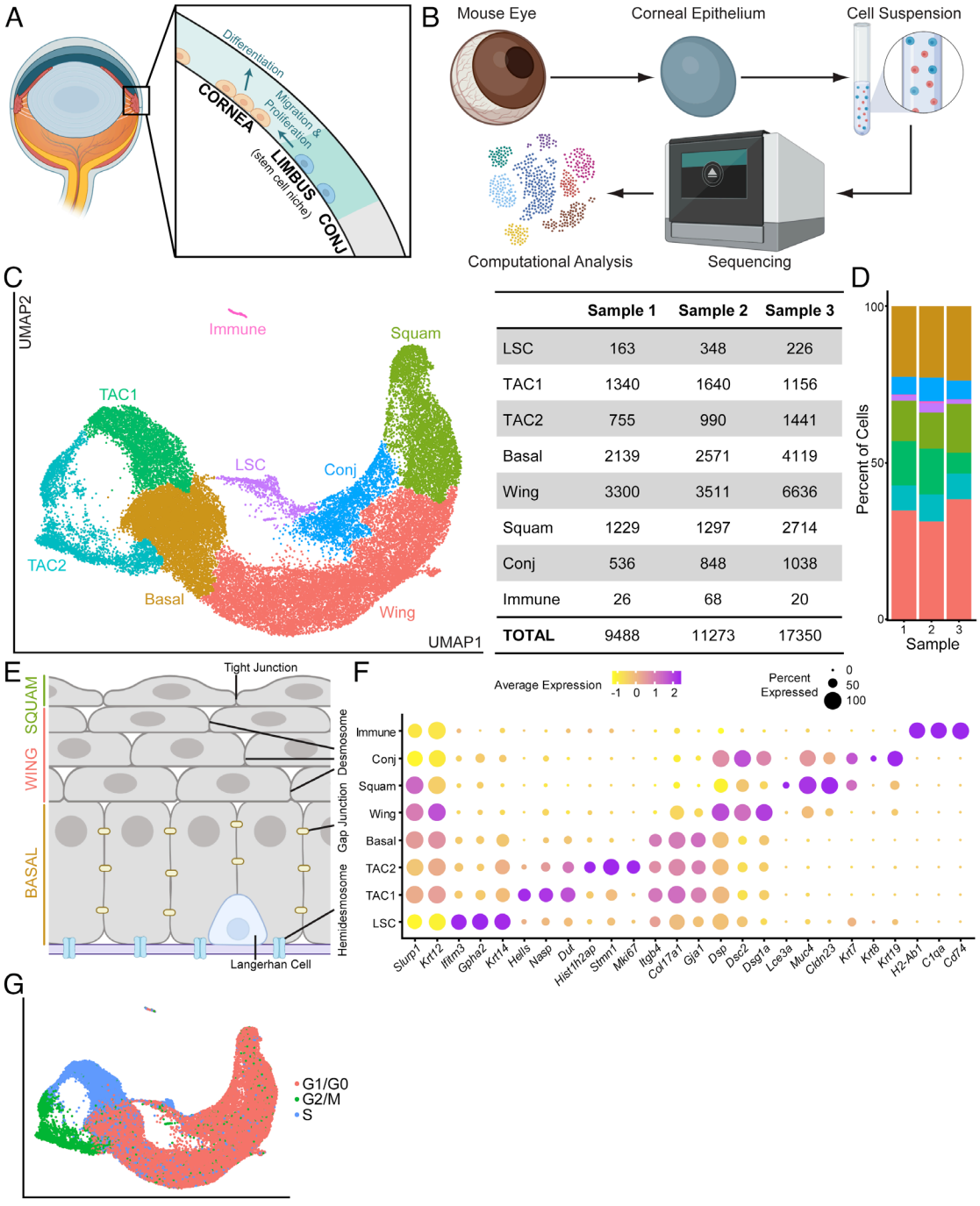

	Sample 1	Sample 2	Sample 3
LSC	163	348	226
TAC1	1340	1640	1156
TAC2	755	990	1441
Basal	2139	2571	4119
Wing	3300	3511	6636
Squam	1229	1297	2714
Conj	536	848	1038
Immune	26	68	20
TOTAL	9488	11273	17350

Fig. 1. Single-cell atlas of the homeostatic mouse corneal epithelium. (*A*) Schematic for canonical model of LSC differentiation (created in BioRender). (*B*) Summary of experimental strategy (created in BioRender). (*C*) UMAP plot of scRNAseq atlas of the mouse corneal epithelium with table delineating cell frequencies for each population (n = 3 independent sequencing experiments). LSC, limbal stem cell; TAC, transit amplifying cell; Squam, squamous; Conj, conjunctiva. (*D*) Stacked bar plot showing relative frequencies for each cell cluster separated by sample. Colors correspond to those in *C*. (*E*) Schematic of cell adhesion molecules defining basal, wing, and squamous cell layers (created in BioRender). (*F*) Dot plot showing marker gene expression patterns. (*G*) UMAP plot showing cell cycle position assigned for each individual cell.

surface stem cell regenerative pathways. Critically, this study also provides insight into expression fidelity of putative LSC markers in nonhomeostatic conditions and is clinically relevant to the treatment of ocular surface disease in humans. The transcriptional programs described here may also have potential broader applicability to our understanding of other epithelial stem cell populations in diverse tissues that accomplish tissue renewal and regeneration.

Results

scRNAseq Captures the Heterogeneity of Corneal Epithelial Cell States in Homeostatic Turnover. We prepared single-cell suspensions of the mouse corneal epithelium by dissecting the eye to isolate the cornea followed by two sequential enzymatic digests. First, enzyme G was used to loosen epithelial–stromal adhesions and cleanly separate the epithelium from the other corneal layers (i.e., stroma + endothelium) (*SI Appendix*, Fig. S1*A*). Then, trypsin was used to dissociate the epithelial sheets into individual cells (*SI Appendix*, Fig. S1*B*), which were then prepared for scRNAseq using the 10x Chromium platform (Fig. 1*B*). We sequenced single-cell preparations of the homeostatic mouse corneal epithelium in three independent experiments, with each sample containing cells from ≥4 pooled mouse corneas (sample details are provided in *SI Appendix*, Fig. S1*C*). In total, after filtering out low-quality

cells and integration to control for experiment-specific variation, we obtained transcriptomes of 38,111 cells across three samples (Fig. 1 *C* and *D* and *SI Appendix*, Fig. S1 *D* and *E*).

Visualization of single-cell transcriptomes in the Uniform Manifold Approximation and Projection (UMAP) space and clustering by the Louvain algorithm identified eight transcriptionally distinct cell states. These cell states appeared with similar proportions in all three sequencing experiments (Fig. 1 *C*–*E* and *SI Appendix*, Fig. S1*D*). Six of these eight cell states represent stages across corneal epithelial differentiation: LSCs, TAC1/2, basal cells, wing cells, and squamous cells. LSCs were characterized by high expression of putative stem cell markers (*Krt14, Ifitm3,* and *Gpha2*) and low expression of differentiation markers (*Krt12* and *Slurp1*), indicating that these likely represent the undifferentiated LSC population (Fig. 1*F*) (1, 5, 9–14). *Krt14* expression was also detected in TACs and basal cells, although at a lower level as compared with LSCs (Fig. 1*F*). The remaining five corneal epithelial cell types showed higher expression of the mature corneal epithelium markers *Krt12* and/or *Slurp1.* Their identities were further inferred based on i) expression of adhesion molecules that roughly define their basal–apical position, ii) cell cycle scoring to identify proliferating cells (i.e., TACs), and iii) marker genes identified agnostically in our scRNAseq dataset. Cells in the basal corneal epithelium are anchored to the basement Bowman layer by hemidesmosomes and connected to adjacent basal cells by gap junctions (Fig. 1*E*) (15). There was high expression of hemidesmosome and gap junction components (*Col17a1*, *Itgb4,* and *Gja1)* in TACs and basal cells (Fig. 1*F*), consistent with the fact that these reside in the basal layer of the corneal epithelium (Fig. 1*A*). TACs were distinguished from resting basal cells by cell cycle scoring and were identified as either TAC1 in the S phase or TAC2 in the G2/M phase (Fig. 1*G*). The distinction between TAC1 and TAC2 may not represent distinct cell populations but likely are proliferating cells at different stages of the cell cycle. Wing cells in suprabasal layers are adjoined by desmosomes with high expression of *Dsg1a, Dsp,* and *Dsc2* (Fig. 1 *E* and *F*). Squamous cells in the most superficial layer express tight junction genes such as *Cldn23* that form an intercellular seal (Fig. 1 *E* and *F*). Squamous cells also expressed *Muc4,* a mucin secreted by surface epithelial cells, and the cornification protein *Lce3a* (Fig. 1*F*). Therefore, we have captured the following corneal epithelial subpopulations: LSCs, TACs, basal cells, wing cells, and squamous cells. These cell clusters in the UMAP space show that LSCs form a continuous trajectory with TACs which connect to basal, wing, and then squamous cells, suggesting that the UMAP embedding faithfully captures canonical corneal epithelial differentiation in homeostasis (Fig. 1*C*).

We corroborated the existence of these distinct transcriptional cell states and their expected in situ localization by validating markers at the protein level using immunohistochemistry. GJA1 was detected throughout the basal epithelium (Fig. 2 *A* and *B*), and DSC2 was detected throughout suprabasal layers (Fig. 2 *A* and *C*). MUC4, a squamous cell marker, was localized only to the most superficial layers of the corneal epithelium (Fig. 2 *A* and *C*). Our scRNAseq dataset suggests that a fraction of the cells in the basal layer should be proliferating TACs. We used confocal microscopy to assess for the proliferation marker Ki67 in the basal epithelium of whole-mount corneas. Ki67 was detected in a subset of basal epithelial cells in the central cornea (Fig. 2 *A* and *D*). The LSC marker IFITM3 was restricted to the basal limbus, the putative stem cell niche, and was absent from the central cornea (Fig. 2 *E* and *F*).

In addition to the six corneal epithelial cell states in our scRNAseq dataset, there was also a small population of immune cells (Fig. 1*C*) likely representing dendritic cells and/or macrophages as indicated by marker genes *Cd74, C1qa,* and *H2-Ab1* (Fig. 1*F*) (16). As expected, there was also a small population of conjunctival epithelial cells characterized by expression of *Krt19, Krt8,* and *Krt7* (Fig. 1 *C* and *F*) (5, 17). These conjunctival cells were localized peripheral to the limbus (Fig. 2 *E* and *F*). The six corneal epithelial, one immune, and one conjunctival cell state(s) constitute all of the cell populations expected to be captured in our sample.

We compared our scRNAseq dataset with two existing datasets for the mouse cornea. We examined the markers for the cell populations reported by Kaplan et al. and found there was very good concordance between ours and their dataset (*SI Appendix*, Fig. S2*A*) (18). A subsequent scRNAseq study by Altshuler and Amitai-Lange et al. revealed that there may be two transcriptionally distinct LSC compartments: one in the inner limbus (*Atf3+/Mt1-2+*) and the other in the outer limbus (*Ifitm3+/Cd63+/Gpha2+*) (5). We examined expression of these and other markers reported by Altshuler and Amitai-Lange et al. (*SI Appendix*, Fig. S2*B*). Again, there was very good agreement for the majority of these marker genes (*SI Appendix*, Fig. S2*B*). Expression of outer LSC markers *Ifitm3, Gpha2,* and *Cd63* coincided with LSCs in our dataset (*SI Appendix*, Fig. S2*B*). However, inner limbal markers *Mt1* and *Mt2* were detected in LSCs, TACs, and basal cells, whereas *Atf3* and *Socs3* were not substantially detected in our dataset (*SI Appendix*, Fig. S2*B*). Our data suggest that there is a single bona fide population of LSCs, but it is possible that sequencing depth precludes identifying LSC subpopulations.

Our homeostatic dataset provides complementary information to existing scRNAseq studies by independently validating cell populations and their markers as well as providing new marker genes. We leveraged our scRNAseq dataset to identify potential new LSC markers. We identified the top 30 up-regulated genes that distinguished LSCs compared with other cell types (*SI Appendix*, Fig. S2*C*). Of these, *Krt17, Fabp5, Id1, Cyp2f2, Serpinb3a, Abi3bp, Ptma, Gas5, Txnip, Fxyd3, Rbp1,* and *Ccnd2* were also expressed substantially in non-LSC cell types (*SI Appendix*, Fig. S2*C*). Many of the remaining 18 genes have been previously reported as LSC markers: *Gpha2, Krt14, Ifitm3,* and *Cd63* (5). We also noticed that some of these LSC markers were also expressed in immune cells (*Apoe, Tmem176a/b, 2410006H16Rik,* and *Cd63)*, consistent with a previous study showing that immune cells regulate the LSC niche (5).

Gene Expression Changes across LSC Differentiation in Homeostasis. We performed supervised pseudotemporal analysis to characterize the gene expression changes throughout canonical LSC differentiation using psupertime (19). We ordered cell states in the following sequence in concordance with the canonical model of LSC differentiation: i) LSCs, ii) TAC1, iii) TAC2, iv) basal cells, v) wing cells, and then vi) squamous cells (*SI Appendix*, Fig. S3*A*). We grouped gene expression patterns into four categories: i) genes that decrease, ii) genes with an early feature (peak or trough), iii) genes with a late peak, and iv) genes that increase (*SI Appendix*, Fig. S3*B*). We believe that these four categories of genes broadly capture different stages of LSC differentiation. For instance, *Krt14* decreases in expression as LSCs progress to TACs (*SI Appendix*, Fig. S3*C*); thus, these reflect markers of stem cell activity, consistent with *Krt14* role in maintaining basal layer cell proliferation (20). Genes with early peaks include the hemidesmosome component *Col17a1* and proliferative marker *Mt2* (*SI Appendix*, Fig. S3*C*); the latter likely reflects activation of proliferation programs in TACs. Increased expression of *Col17a1* in TACs as compared with LSCs could reflect de novo synthesis of hemidesmosome components as they extend centripetally toward the center of the cornea. Differentiation is achieved as basal cells migrate superficially, and wing cells exhibit peak expression of *Hopx* (*SI Appendix*, Fig. S3*C*), which has been shown to regulate differentiation in other epithelial tissues (21). Last, genes that maintain high expression in squamous cells include *Cryab* that helps to maintain a transparent ocular surface (22), *Muc4* to help provide surface lubrication (23), and *Fth1* which protects corneal epithelial DNA from UV damage (24) (*SI Appendix*, Fig. S3 *B* and *C*).

Gene Regulatory Networks (GRNs) across LSC Differentiation in Homeostasis. GRNs represent transcription factors and their target genes, and we sought to identify the key regulators responsible for coordinating the broad transcriptional changes that occur across corneal epithelial differentiation in homeostasis. We used single-cell regulatory network inference and clustering (SCENIC) to discover

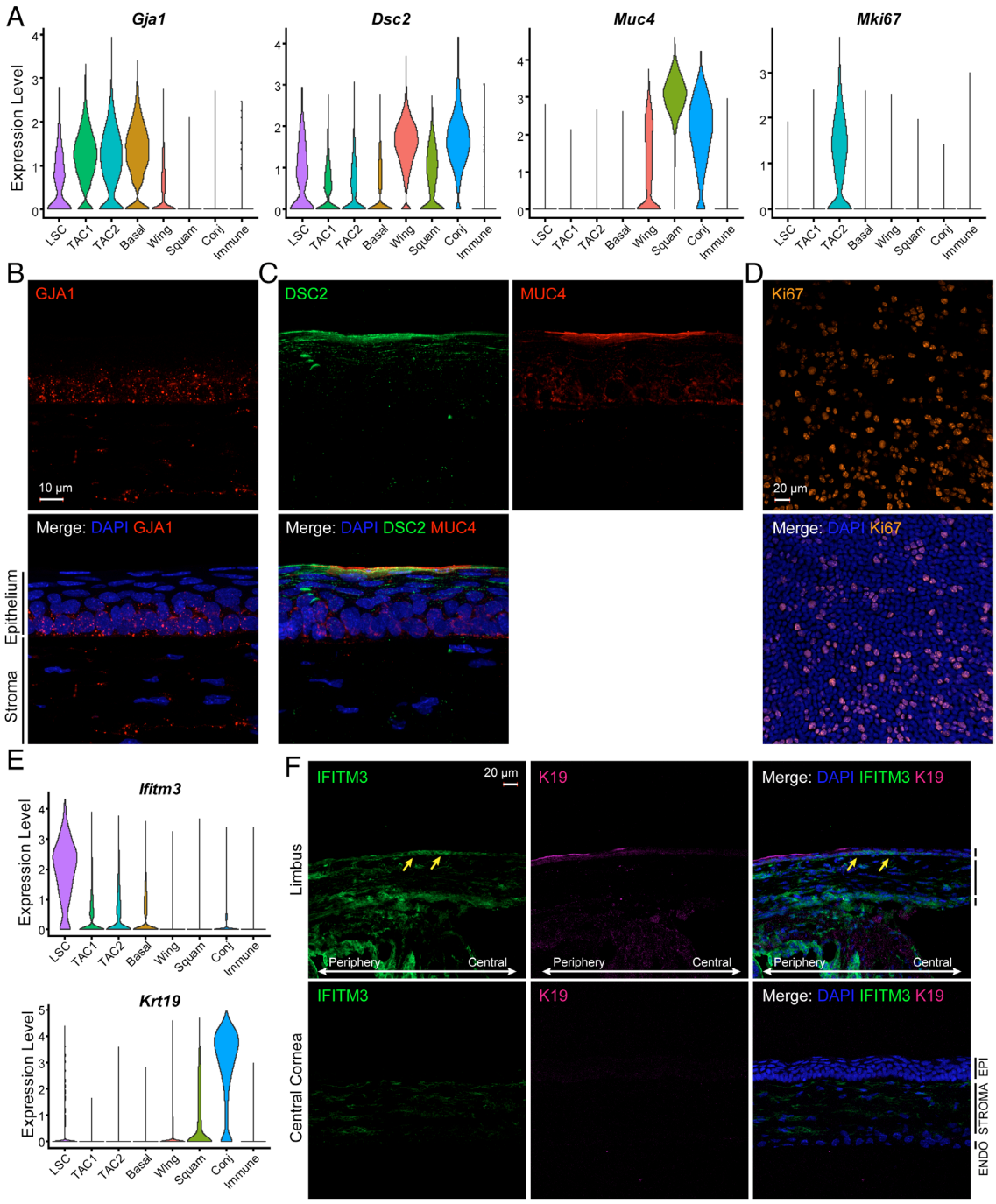

Fig. 2. Markers for cell types in constitutive corneal epithelial renewal. (*A*) Violin plots showing expression of *Gja1, Dsc2, Muc4,* and *Mki67*. (*B* and *C*) Immunostaining of GJA1, DSC2, and MUC4 in the central cornea. Images reflect maximum projection across the entire thickness of the tissue section. (*D*) Ki67 immunostaining in the whole-mount cornea. This image was created by maximum projection of a Z-stack including only the basal layer of epithelial cells. (*E*) Violin plots showing expression of *Ifitm3* and *Krt19*. (*F*) Immunostaining of the cornea for IFITM3 and K19. (Scale bars are the same for images in *B* and *C*.)

the GRNs characterizing cell states in the corneal epithelium (25, 26). Hierarchical clustering of cell populations based on these GRNs indicated that epithelial cells in the basal cell compartment (i.e., LSCs, basal cells, and TAC1/2) have distinct transcriptional regulation from other more differentiated epithelial cells (i.e. squamous and wing) (Fig. 3*A*). There also appeared to be groups of GRNs that broadly define stemness, proliferation, differentiation, and function of ocular surface squamous cells. Regulons of stem cell activity include *Trp63*, *Sox9*, and *Cebpd* (Fig. 3 *B* and *C*), some of which have been described to be transcription factors important for stem activity in corneal and other epithelial tissues (27–29). The putative stem cell marker *Trp63* demonstrated activity not only in LSCs but also in TACs and some basal cells (Fig. 3*B*), consistent with protein localization detected by immunostaining (*SI Appendix*, Fig. S4). TACs are characterized by regulators of cell cycle entry and DNA repair such as *Ezh2*, *E2f8*, and *Tfdp1* (Fig. 3 *B* and *C*). The factors important in early corneal epithelial differentiation can be identified by those with increased activity in wing cells such as *Kdm5b, Xbp1,* and *Nfe2l3* (Fig. 3 *B* and *C*), some of which have been reported to regulate differentiation in corneal or other epithelial tissues (30). Finally, transcription factors important in late-stage differentiation of squamous cells include *Prdm1*, *Irf7,* and *Srf* (Fig. 3 *B* and *C*). *Prdm1* regulates type III interferon responses (31) shown to be responsible for immune responses to viral pathogens including Zika and herpes simplex 1 viruses (32). Furthermore, *Srf* is known to be important in forming cell–cell adhesions (33), a critical aspect

of protective barrier function by the ocular surface. Therefore, we are able to identify not only transcriptional programs of stemness, proliferation, and differentiation but also those maintaining corneal function as a protective barrier.

Corneal Epithelial Cell States Are Maintained Transcriptionally in Resting Aged and Diabetic Cornea. We have delineated the transcriptional hallmarks of LSC differentiation in the resting cornea, but the role, activation, and/or dysfunction of LSCs in nonphysiologic conditions remains poorly understood. Previous studies have demonstrated exhaustion of numerous stem cell populations with age (34). Indeed, LSC dynamics were also found to be altered during aging with streaks of centripetally migrating LSCs/TACs increasing in width and decreasing in number (35, 36). An additional study demonstrated that aging human LSCs exhibit decreased colony-forming efficiency (37). Therefore, to test the hypothesis that LSC differentiation may become perturbed in aged mice, we performed scRNAseq to capture LSC differentiation in the young (11 wk old) vs. aged (≥18 mo old) corneal epithelium. Based on our scRNAseq data, all cell states from homeostatic turnover were maintained in aged mice (*SI Appendix*, Fig. S5 *A–C*). Their transcriptomes were also largely preserved with Pearson correlation coefficients ranging from 0.99 to 1.0 (*SI Appendix*, Fig. S5*D*). We determined differentially expressed genes (DEGs) in each cell population (i.e., $|\log_2 FC| \geq 1$) and found only a few genes to be changed across aging (*SI Appendix*, Fig. S5*E*). Therefore, we were not able to capture substantial age-related stem cell exhaustion at the transcriptional level in the resting mouse corneal epithelium, consistent with previous reports that limbal tissues sourced from older donors can be suitable for LSC transplantation (38, 39).

Another context in which corneal epithelial maintenance may be dysfunctional is diabetes. The diabetic corneal epithelium exhibits increased fragility, recurrent ulcers and erosions, edema, keratitis, and delayed healing (40–42). These corneal manifestations of systemic hyperglycemia are also seen in animal models of diabetes, including both streptozotocin (STZ)-induced hyperglycemia and $Lepr^{db/db}$ diabetic mice (43, 44). Therefore, we sought to determine whether hyperglycemia perturbs the LSC compartment in mice. We induced hyperglycemia using the pancreatic beta cell toxin STZ and measured blood glucose weekly to certify chronic hyperglycemia was maintained (i.e., >250 mg/dL; *SI Appendix*, Fig. S6*A*). We performed scRNAseq of the corneal epithelium after 12 wk of hyperglycemia and compared the corneal epithelium with euglycemic controls. Twelve weeks of hyperglycemia is sufficient to incur ocular surface sequelae of diabetes as described in previous studies (45–53). Even after extended systemic hyperglycemia, the cell heterogeneity of the corneal epithelium was conserved (*SI Appendix*, Fig. S6 *B–D*). Similar to aging, transcriptomes of each cell population were still largely maintained in hyperglycemia with correlation coefficients ranging from 0.99 to 1.0 in diabetic corneas (*SI Appendix*, Fig. S6*E*). There were only two DEGs (i.e., $|\log_2 FC| > 1$) (*SI Appendix*, Fig. S6*F*). Our data therefore imply that dysfunction of LSC differentiation does not dramatically contribute to diabetic keratopathy in the otherwise uninjured cornea, at least at the transcriptional level.

Aqueous Tear–Deficient DED Activates an Adaptive Regenerative Program. We have provided evidence that the cell states characterizing the homeostatic corneal epithelium are largely maintained at the transcriptional level even after aging or extended hyperglycemia. We next hypothesized that the corneal epithelium may activate wound healing programs in ocular surface diseases characterized by epithelial defects and injury. DED results from disruptions to the ocular tear film and affects ~20% of individuals impacting their quality of life and can progress to vision loss or even blindness if left untreated (8). The tear film comprises the following three components: i) aqueous secretions from lacrimal glands, ii) lipid component from Meibomian glands, and iii) mucous layer produced by goblet cells. If the stability of the tear film is compromised by deficiency of any of these components, the ocular surface becomes dry and irritated. Patients may have isolated DED, but it can also arise with other multisystem diseases such as in Sjögren's syndrome or graft-vs.-host disease in which there are lacrimal gland inflammation and dysfunction (8).

To study the effects of DED on the transcriptional heterogeneity of the corneal epithelium, we surgically excised the right extraorbital and intraorbital lacrimal glands in mice (54), with the left side serving as the control eye (Fig. 4*A*). At 1 wk after excision of lacrimal glands, we confirmed the presence of DED-induced corneal epitheliopathy by fluorescein staining, which revealed patchy areas of ocular surface injury in all eyes used for further analysis (Fig. 4*B*). Nine days after lacrimal gland excision, we isolated corneal epithelial cells from control and dry eyes pooled from n = 7 mice and performed scRNAseq. We excluded one dry eye sample from study because it suffered collateral injury during excision of the intraorbital lacrimal gland. Our scRNAseq dataset of DED demonstrated that along with immune and conjunctival cells, all of the cell populations of homeostatic renewal were conserved in DED: LSCs, TAC1/2, basal cells, wing cells, and squamous cells (Fig. 4 *C–E*). However, there was activation of new cell states (Fig. 4*C*, cell types in bold with asterisk). These DED-elicited cells were very rare in control eyes (total 172/17,465 = 1.0%) but dramatically expanded >10-fold to 11% (1,793/16,420) of the corneal epithelial cell population in DED. Based on moderate *Krt12* expression and lower *Krt19* expression (Fig. 4*D*), these DED-elicited cells appear to be corneal epithelial cells. This DED model likely affects predominantly the cornea due to protection of the conjunctiva by the eyelid. We were able to identify five cell states elicited by DED including LSC-like cells (LSC*), TACs (TAC1*/TAC2*), wing cells (wing*), and squamous cells (squamous*) based on the same markers used to identify cell types in homeostasis (Fig. 4 *D* and *E*). The heterogeneous composition of these DED-induced cell states seems to roughly mirror the canonical sequence of LSC differentiation in homeostasis. Taken together, these results indicate that although the constitutive transcriptional program seen in homeostatic tissue turnover is maintained in dry eye–induced epitheliopathy, there is also activation of a disease-specific regenerative response. We term this DED-activated program as adaptive regeneration.

Constitutively Renewing Corneal Epithelial Cell Types Are Conserved in DED. To shed further light into the transcriptional changes associated with DED epitheliopathy, we first evaluated the cell types that were conserved from homeostatic turnover (i.e., LSCs, TAC1/2, basal cells, wing cells, and squamous cells). The transcriptional signature of these constitutive cell types in control vs. dry eye is largely unchanged, with Pearson correlation coefficients ranging from 0.98 to 1.0 (Fig. 5*A*). To more specifically define these changes, we assessed for DEGs ($|\log_2 FC| \geq 1$). We found that there were 11 unique genes up-regulated and one gene down-regulated in DED across all of the conserved cell types (Fig. 5 *B* and *C*), with many of these having been previously associated with wound healing in other epithelial compartments. While some of these changes were cell type-specific, other changes were conserved responses across multiple cell types (Fig. 5*B*). For instance, *Fabp5* was up-regulated in all six cell types (Fig. 5 *B* and *C*), consistent with upregulation that is seen in the psoriatic epidermis (55). The putative LSC marker *Krt14* was up-regulated in basal cells, TACs, and wing cells (Fig. 5 *B* and *C*), suggesting an increased stem-like transcriptional signature in these cells. The cystatin gene *Cstdc5* was up-regulated in basal cells and TACs (Fig. 5 *B* and *C*). *Krt16* was up-regulated in TACs, wing cells, and squamous cells similar to upregulation that is also seen in the wounded epidermis (Fig. 5 *B* and *C*) (56). The keratinocyte envelope protein *Sprr1a* was up-regulated in wing and squamous cells (Fig. 5 *B* and *C*) similar to upregulation that was recently reported in an acute model of intestinal injury (57). The remaining seven genes were dysregulated in a cell type–specific manner. In LSCs, *Clu* and *Ly6a* were up-regulated, while *Aqp5* was down-regulated (Fig. 5 *B* and *C*). Both *Clu* and *Ly6a* are up-regulated in acute villus injury (57, 58) (Fig. 5 *B* and *C*). In TAC2s, *Krt16* binding partner *Krt6a* was up-regulated (56) (Fig. 5 *B* and *C*). In wing cells, *Ifitm1* was up-regulated (Fig. 5

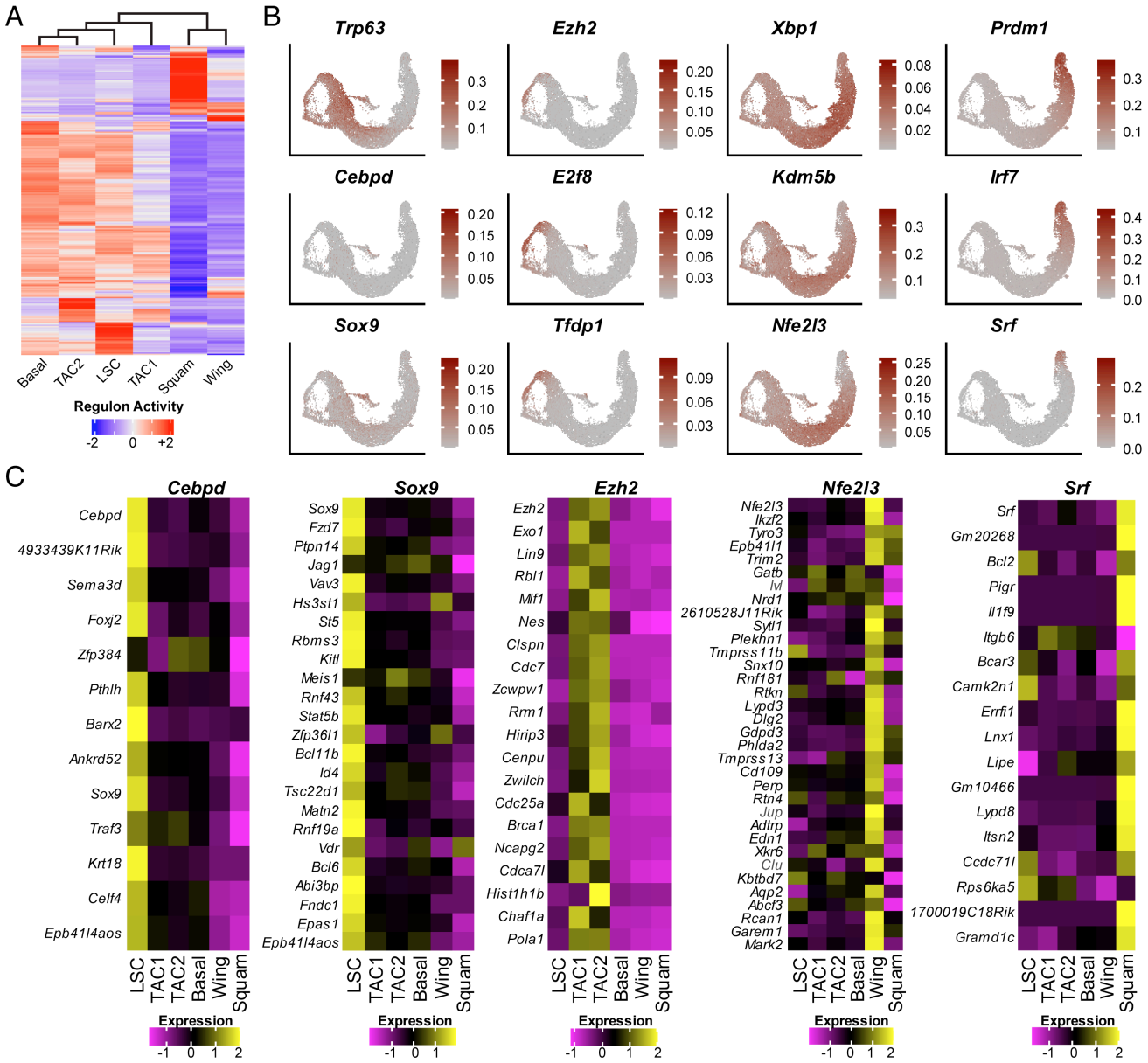

Fig. 3. Gene regulatory networks characterizing corneal epithelial cell types in homeostasis. (*A*) Heat map depicting GRN activity in each cell cluster. Each row is a single GRN, and hierarchical clustering of cell types was performed based off of GRN activity. (*B*) UMAP plots of GRN activity for transcription factors that may define each stage of differentiation. (*C*) Heat maps show average expression of transcription factors and their target genes for each cell cluster.

B and *C*). In squamous cells, *Cnfn* and *Cdsn* were up-regulated, which are both members of the cornification cell envelope (Fig. 5 *B* and *C*). In general, there were no more than five DEGs for each conserved cell type, suggesting that the constitutive renewal program is largely maintained in DED. This is likely due to the fact that ocular surface injury in this DED model is regional with areas of the intact epithelium (Fig. 4*B*).

Transcriptional Signature of Adaptive Regeneration Activated by Aqueous Tear–Deficient DED. We next determined the unique transcriptional signature of the adaptive cell responses activated in DED (i.e., LSC*, TAC1/2*, wing*, and squamous*). We assessed for genes distinguishing DED-elicited cell states from their constitutive counterparts (i.e., we compared LSCs vs. LSCs*; TAC1 vs. TAC1*; TAC2 vs. TAC2*; wing vs. wing*; squamous vs. squamous*) (*SI Appendix*, Fig. S7*A*). In total, there were 303 unique dysregulated genes across these five comparisons with $|\log_2 FC| > 1$ (Fig. 5*D*).

We first evaluated which, if any, genes could serve as markers that globally distinguish adaptive regeneration in disease from constitutive tissue turnover. Therefore, we identified genes that were dysregulated in the majority of DED-elicited cell types (Fig. 5 *D* and *E*). There were 40 unique genes that were identified as DEGs in ≥3/5 comparisons (Fig. 5*D* and *SI Appendix*, Fig. S7*B*). In addition to the 2 potential LSC markers *Lgals7* and *Krt14*, there were 12 genes that appeared to broadly distinguish DED-elicited cell types from cell types conserved from homeostasis. Four of these transcripts displayed reduced expression in DED: *Cdo1*, *Hlf, F3,* and *Adh7* (Fig. 5*E*). *Hlf, F3,* and *Adh7* were not expressed in squamous cells but were expressed in all other homeostatic corneal epithelial types. We also identified eight markers that were globally enriched in DED-elicited cell types: *Serpinb5, Pkm, Ifngr1, Stom, Urah, Rbp1, Clu,* and *Fabp5* (Fig. 5*E*). Therefore, we have identified potential markers that broadly distinguish cell types that contribute to constitutive tissue turnover from cell types that accomplish adaptive regeneration in DED (Table 1).

To delineate the unique transcriptional signature of DED-elicited proliferating cell states, we identified the overlap in markers for TAC1* and TAC2*, which were in the S phase and G2/M phase, respectively (Figs. 4*E* and 5*D*, and *SI Appendix*, Fig. S7*C*). There

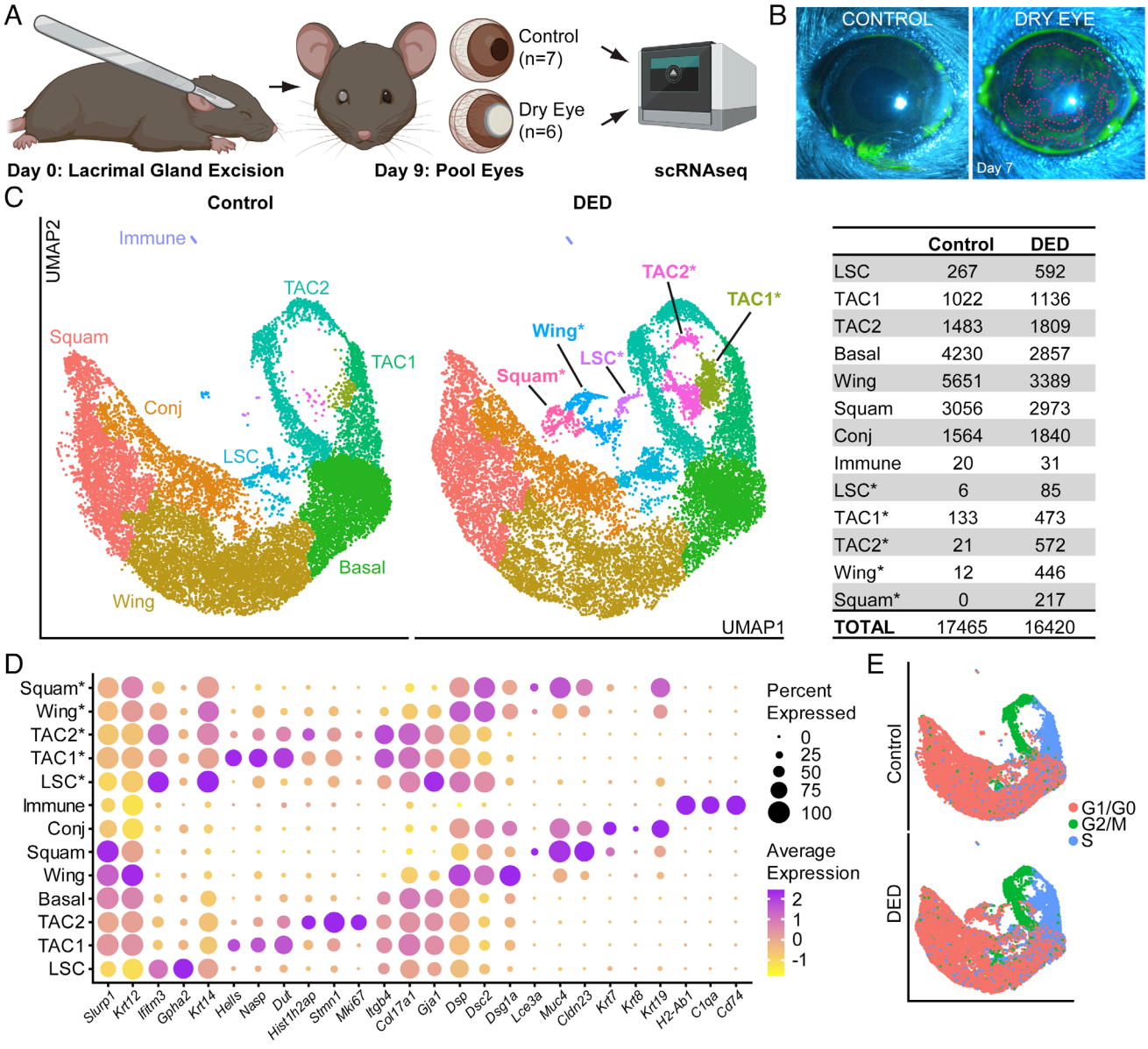

	Control	DED
LSC	267	592
TAC1	1022	1136
TAC2	1483	1809
Basal	4230	2857
Wing	5651	3389
Squam	3056	2973
Conj	1564	1840
Immune	20	31
LSC*	6	85
TAC1*	133	473
TAC2*	21	572
Wing*	12	446
Squam*	0	217
TOTAL	17465	16420

Fig. 4. Single-cell atlas of the corneal epithelium in a mouse model of DED. (*A*) Schematic of experimental approach (created in BioRender). (*B*) Fluorescein staining of ocular surface in control vs. DED at 7 d after lacrimal gland excision. The magenta dashed outline circumscribes areas of epithelial injury. (*C*) UMAP plots of corneal epithelial cell populations in control and DED with table delineating cell cluster frequencies. LSC, limbal stem cell; TAC, transit amplifying cell; Squam, squamous; Conj, conjunctiva; * denotes cell types elicited in DED. (*D*) Dot plot showing marker gene expression patterns. (*E*) UMAP plot of cell cycle positions assigned to each individual cell.

were 24 overlapping genes identified, with three of these (*Mt1, Mt2,* and *Sparc)* appearing to be markers for both TAC1* and TAC2* cells (Fig. 5*F*). *Mt1* and *Mt2* were expressed in homeostatic TAC1/2 cells, although at a lower level compared with DED-elicited TAC1/2* cells (Fig. 5*F*). Thus, *Sparc* is the most specific transcriptional marker of DED-elicited proliferating cell states and may be a marker of adaptive proliferation activated in DED (Fig. 5*F*).

To define the unique transcriptional signature of DED-elicited differentiated cell states, we identified the overlap in DEGs for wing* and squamous* cells (Fig. 5*D* and *SI Appendix*, Fig. S7*D*). There were 32 overlapping genes, of which 13 genes appeared to distinguish DED-elicited differentiated cell types from differentiated cells that exist in homeostasis (Fig. 5*F*). Wing and squamous cells in homeostasis had high expression of *Id2* and *Ttc36,* whereas wing* and squamous* cells induced in DED exhibited high expression of *Il1f9, Ceacam1, Shroom3, Ecm1, Spink5, Aldh1a3, Sprr1b, Cnfn, Sprr1a, S100a9,* and *Krt16* (Fig. 5*F*). Due to its highest 5.6 to 5.8 $\log_2$ (fold change), we chose *Krt16* as the defining marker of DED-elicited differentiated cell states. We suggest that *Krt16* activation could reflect unique differentiation programs i) to help protect the ocular surface in disease scenarios and/or ii) that are only apparent when the corneal epithelium undergoes accelerated differentiation in the presence of injury.

Finally, we noticed that some putative LSC markers expanded their expression to DED-elicited adaptive cell states (Fig. 5*E* and *SI Appendix*, Fig. S7 *B–D*). Therefore, we assessed which stem cell markers remain restricted to bona fide LSCs in disease and which markers were promiscuous with expression in DED-elicited cell states. The putative LSC markers *Krt14, Lgals7,* and *Ifitm3* demonstrated dramatically expanded expression to several DED-elicited cell types (Fig. 5*G*). *Igfbp2/7* showed expanded expression to the DED-elicited LSC* population but not others. Therefore, our scRNAseq dataset allows for the classification of putative LSC markers as 1) stringent if their expression remains completely restricted to bona fide LSCs in disease, 2) semistringent if their expression is nonspecific to one other cell population, or 3) labile if their expression expands to several other populations in DED (Table 2).

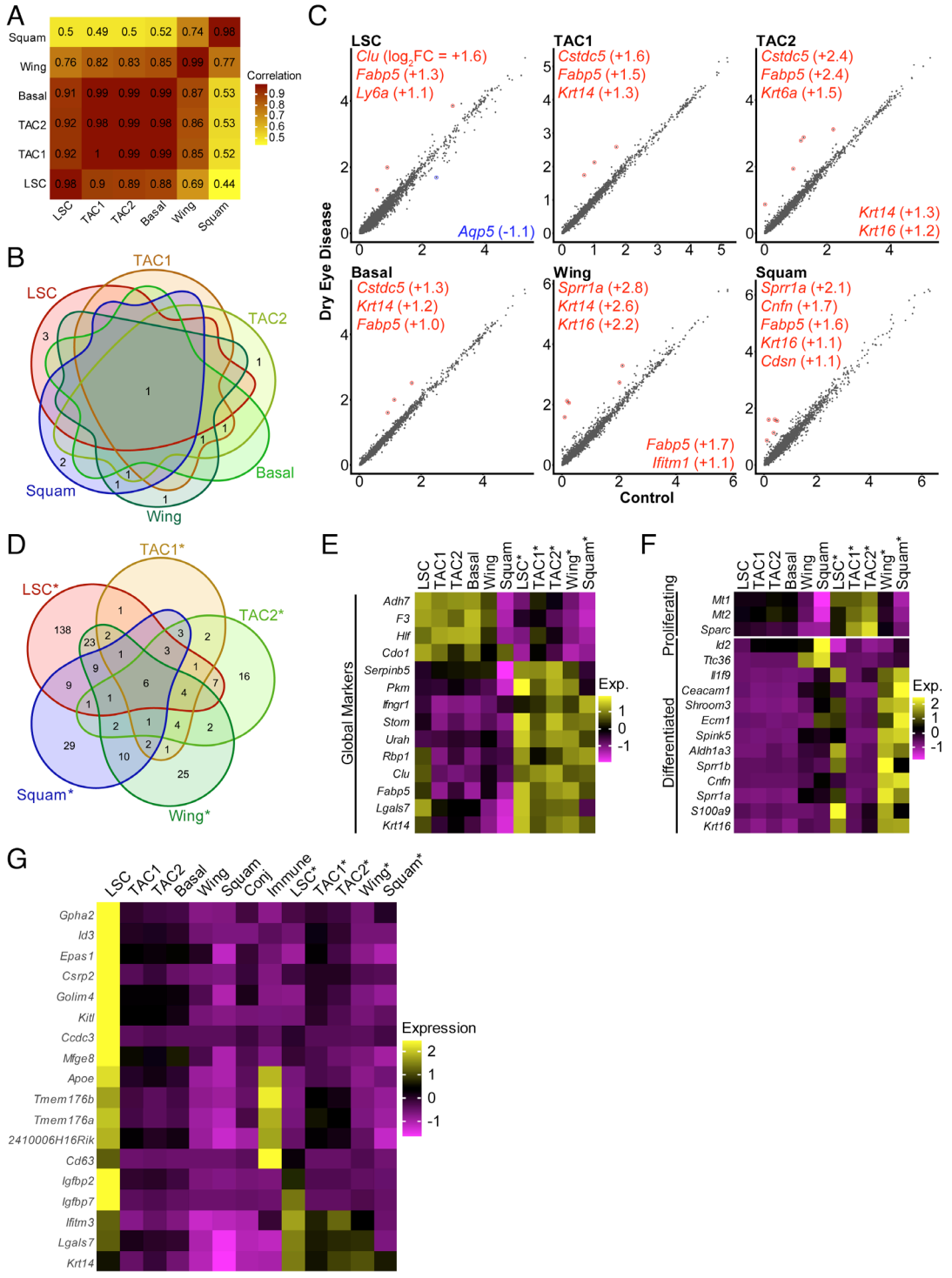

Fig. 5. Transcriptional signature of adaptive corneal epithelial regeneration activated in DED. (*A*) Correlation matrix comparing transcriptomes of cell types in DED that are conserved from homeostasis. (*B*) Venn diagram showing the overlap of genes dysregulated in DED for cell types conserved from homeostasis. (*C*) Scatterplots compare the expression of genes in cell populations that are present in both control and DED. Listed genes are significantly dysregulated (i.e., adjusted *P* value < 0.05; $|\log_2 FC| \geq 1$). Genes that are up-regulated are listed in red and down-regulated in blue. (*D*) Venn diagram showing the overlap of genes that define DED-elicited cell types compared with their constitutive counterparts (i.e., LSC* vs. LSC; TAC1* vs. TAC1; TAC2* vs. TAC2; wing* vs. wing; squamous* vs. squamous). (*E*) Heat map depicts the average expression of genes that broadly distinguish cell types of constitutive turnover in homeostasis vs. adaptive regeneration activated in DED. (*F*) Heat map depicting the average expression of genes that distinguish proliferating and differentiated cells in homeostasis vs. DED. (*G*) Heat map of average expression of LSC markers in constitutive and DED-elicited cell types.

Gene Regulatory Networks Characterizing DED–Elicited Response. To better define the transcriptional regulation of DED-induced cell states, we also assessed for GRNs whose activity is enriched in these cells. Strikingly, hierarchical clustering based on GRN activity revealed that DED-elicited cell populations were transcriptionally regulated very similarly to their homeostatic counterpart (*SI Appendix*, Fig. S7*E*). For example, TAC1* and TAC2* cells were positioned adjacent to TAC1 and TAC2 cells. There also appeared to be GRNs that were enriched in DED-elicited cells, including the FOSB GRN, which has been reported to have a role in epithelial differentiation in other tissues (66), again pointing to activation of epithelial differentiation programs that are uniquely activated in DED.

Role of SPARC in Corneal Epithelial Wound Healing. Our scRNAseq data indicate that SPARC is a marker of adaptive regeneration that is activated when the corneal epithelium experiences severe desiccative

stress. Since there may be conserved transcriptional programs activated in both DED and injury to the corneal epithelium, we hypothesized that SPARC expression may also be induced during wound healing. In mice, we mechanically debrided a 2-mm-diameter circle from the central corneal epithelium with an AlgerBrush II rotating burr. One day after injury, we found that SPARC protein was strongly expressed at the leading edge of the corneal epithelial wound, while it was completely absent in the uninjured corneal epithelium (Fig. 6 *A* and *B*). At this early time point following injury, SPARC is localized mostly intracellularly prior to secretion. Therefore, activation of SPARC appears to be a conserved response of corneal epithelial cells in DED, injury, and potentially other perturbations to the ocular surface.

We next sought to elucidate the mechanistic effects of SPARC, a secreted protein, on corneal epithelial cells. We performed RNA sequencing to identify transcriptional changes when human corneal epithelial cells (hTCEpi) are incubated with SPARC protein comparing control cells with cells treated with 0.05, 0.50, or 5.00 μg/mL SPARC for 24 h (n = 5/group). We obtained an average of 36.5 million reads per sample, and of these, an average of 36.0 million reads (98.6%) mapped to the human genome. We performed DEG analyses to compare control vs. 0.05 μg/mL SPARC, control vs. 0.50 μg/mL SPARC, and control vs. 5.00 μg/mL SPARC. We found that there was a dose-dependent effect on the number of DEGs with FDR < 0.05 (110 DEGs for 0.05 μg/mL, 554 DEGs for 0.50 μg/mL, and 2,631 DEGs for 5.00 μg/mL). Of the 2,631 genes dysregulated by treatment with the highest SPARC concentration, 68 had $|\log_2 FC| > 1$ (Fig. 6*C*). In order to evaluate for any dose dependency in these 68 genes, we identified which—if any—overlapped with the 554 DEGs for control vs. 0.50 μg/mL SPARC and the 110 DEGs for control vs. 0.05 μg/mL SPARC. Out of the 68 genes dysregulated by the highest SPARC concentration, 19 of these were also dysregulated by the intermediate SPARC concentration, and three were also dysregulated by the lowest SPARC concentration (Fig. 6*C*). *FN1, CCDC80, PMEPA1, FLRT2, AC037198.1, THBS1, ITGB6, SERPINE1,* and *TGFBI* demonstrated a clear dose-dependent effect on gene expression in response to SPARC treatment (Fig. 6*C*). Many of these genes have been previously reported to become activated during corneal injury (67), and we found that along with SPARC, FN1 was also strongly expressed at the leading edge of corneal epithelial injury in mice (Fig. 6*D*). Taken together, our results support that SPARC may be a key gene in coordinating the conserved corneal epithelial response under nonhomeostatic conditions.

To test the role of SPARC in epithelial wound healing, we performed a scratch assay with hTCEpi cells comparing untreated cells with SPARC-treated cells. This assay compares how quickly cells reestablish confluency following a mechanical scratch that creates a gap in a monolayer of confluent cells. Compared with untreated cells, cells treated with SPARC showed increased wound closure at 24 h (Fig. 6 *E* and *F*). We quantified the percentage of scratch area remaining, and there was a statistically significant difference between the four treatment groups at 24 h after scratch (Brown–Forsythe ANOVA test, omnibus P value < 0.01). Specifically, the cells treated with 5 μg/mL SPARC had less scratch area remaining compared with all other treatment groups (Fig. 6*F*), and there also seemed to be a trend indicating a dose-dependent effect of SPARC on wound closure. Therefore, SPARC accelerates corneal epithelial scratch closure.

Discussion

Here, this series of scRNAseq experiments captures the full heterogeneity of the corneal epithelial cell types in homeostasis, aging, diabetes, and DED, forwarding our understanding of a poorly defined yet critically important stem cell population and its differentiation. In homeostasis, we robustly capture all of the cell types that contribute to constitutive renewal of the resting cornea. Our dataset suggests that there is a single population of bona fide LSCs that give rise to proliferating TACs, which differentiate into wing and squamous cells. There also seems to be a population of nonstem/proliferating basal cells. We provide independent validation of previously reported LSC markers and provide others to contribute to the long-standing search for LSC markers. We also clearly show that there appears to be 3 transcriptionally distinct populations of cells in the basal layer: TAC1, TAC2, and basal cells. Both TAC populations are proliferating with cell cycle scoring indicating status in the S phase or G2/M phase. Leveraging our scRNAseq dataset of homeostatic differentiation, we are also able to identify genes and gene networks potentially regulating different stages of homeostatic LSC differentiation. Genetic or pharmacologic manipulation of these genes and/or gene networks of interest could shed further light into the role of these in the constitutive renewal of the corneal epithelium.

Furthermore, our scRNAseq data of aged and diabetic mice indicate that even after extended hyperglycemia or aging, if the ocular surface remains uninjured, populations of stem cells through mature corneal epithelial cell types mirror physiologic conditions. Lack of age-related changes in the mouse corneal epithelium is consistent with previous reports indicating that LSC grafts from elderly donors can be suitable for transplantation (38, 39). We found that diabetes does not substantially perturb resting (i.e., noninjured) corneal epithelial cells at the transcriptional level. Instead, diabetic keratopathy may be driven by i) dysfunction of LSC activation when the corneal surface is injured, ii) perturbations to proteins or other non-mRNA molecules, and/or iii) cell types or noncellular components that are not captured well in our scRNAseq workflow (e.g., nerves, extracellular matrix, and immune cells).

More importantly, our dataset reveals the reconfiguration of the corneal epithelial transcriptional landscape that occurs in DED. We show that all cell types that accomplish constitutive renewal in homeostasis are maintained in DED. However, there was also activation of five disease-specific cell responses—LSC*, TAC1*, TAC2*, wing*, and squamous* cells. These appear to be a rough facsimile of the cell types observed in homeostatic turnover, suggesting that this is an adaptive program of regeneration that is activated in DED, which we term adaptive regeneration. The existence of both

Table 1. Constitutive corneal epithelial renewal in homeostasis vs. adaptive regeneration in DED

	Constitutive tissue renewal	Adaptive regeneration
Cell types	LSCs, TAC1/2, basal cells, wing cells, and squamous cells	LSCs*, TAC1*/2*, wing* cells, and squamous* cells
Homeostasis	+++	-
Aging (uninjured)	+++	-
Diabetes (uninjured)	+++	-
Aqueous tear–deficient DED	++	+
Global marker(s)	*Cdo1*, *Hlf**, *F3**, and *Adh7**	*Serpinb5, Pkm, Ifngr1, Stom, Urah, Rbp1, Clu,* and *Fabp5*
Marker specific to proliferating cells (TAC1/2 or TAC1*/2*)	ND†	*Mt1*‡, *Mt2*‡, and ***Sparc***
Marker specific to differentiated cells (wing/squamous or wing*/squamous*)	*Id2* and *Ttc36*	*Il1f9, Ceacam1, Shroom3, Ecm1, Spink5, Aldh1a3, Sprr1b, Cnfn, Sprr1a, S100a9,* and *Krt16*

*Expressed minimally in squamous cells.
†None determined.
‡Expressed in TAC1/2, although at a lower level than TAC1/2*.LSC, limbal stem cell; TAC, transit amplifying cell.Comparison of constitutive tissue renewal vs. adaptive regeneration including cell states involved, presence/absence in homeostasis and disease models, and marker genes. Gene in bold were validated in corneal epithelial wound healing by immunohistochemistry in the current work.

Table 2. LSC marker expression fidelity

	Stringent, semistringent, or labile	Cell type promiscuity	Previous studies
Gpha2	Stringent	ND*	(5, 9, 59–61)
Id3	Stringent	ND*	(5, 60, 62, 63)
Epas1	Stringent	ND*	(62)
Csrp2	Stringent	ND*	
Golim4	Stringent	ND*	
Kitl	Stringent	ND*	(64)
Ccdc3	Stringent	ND*	
Mfge8	Stringent	ND*	
Apoe	Semistringent	Immune	Up-regulated in cluster 10 of ref. 62
Tmem176a/b	Semistringent	Immune	
2410006H16Rik	Semistringent	Immune	
Cd63	Semistringent	Immune	(5)
Igfbp2/7	Semistringent	LSC*	
Ifitm3	Labile	LSC*, TAC1/2*, and wing* cells	(5)
Lgals7	Labile	LSC*, TAC1/2*, and wing* cells	
Krt14	Labile	LSC*, TAC1/2*, wing* cells, and squamous* cells	Leaky expression to other cells in basal layer after wound healing (65)

*None determined.LSC, limbal stem cell; TAC, transit amplifying cell.We classified putative LSC markers based on their expression stringency in homeostasis and disease models.

constitutive renewal in homeostasis and adaptive responses activated by injury is also seen in other tissues that undergo homeostatic turnover (57). It remains unknown whether bona fide LSCs give rise to the entire adaptive regenerative program or if there is a coordinated transcriptional shift of the cells from constitutive tissue renewal. The expression of LSC markers *Ifitm3* and *Krt14* in DED-elicited cell types is weak circumstantial evidence that these disease-induced cell populations are derived from the bona fide LSC population. Although we did not detect substantial changes in the corneal epithelium in aging or diabetes, these were performed in resting (i.e., noninjured) tissue. It remains possible that the activation of this adaptive program may become dysfunctional in aging and/or diabetes. Further study is needed to determine whether or not adaptive differentiation is perturbed in these or other pathological contexts that involve the ocular surface.

We leveraged our scRNAseq to determine DEGs that broadly distinguish adaptive regeneration from constitutive tissue renewal in the corneal epithelium (Table 1). Globally, constitutive tissue renewal can be characterized by expression of *Adh7, Cdo1, F3,* and *Hlf,* whereas adaptive regeneration has high expression of *Fabp5, Clu, Rbp1, Urah, Stom, Ifngr1, Pkm,* and *Serpinb5 (*Table 1). *Adh7* is a possible target of the LSC marker P63 (68) and has also been previously reported to be dysregulated in patients with aniridic keratopathy from *PAX6* haploinsufficiency (69). Of the markers for adaptive corneal epithelial regeneration activated by DED, *Fabp5* and *Pkm* have been shown to be up-regulated in the psoriatic epidermis (70, 71). *Clu* was up-regulated in intestinal epithelial cells in an acute villus injury model (57). *Urah* encodes an enzyme involved in urate metabolism. Urate generated from purine metabolism is an alarmin that triggers inflammation and wound healing responses (72). Thus, it is conceivable that purines released from corneal trauma generate urate that contributes to activation of injury response pathways. *Rbp1* was up-regulated after epidermal injury in rats (73), and *Serpinb5* has been previously reported to regulate corneal stromal wound healing (74). Thus, further investigation is warranted regarding these genes' roles in constitutive corneal epithelial turnover and wound healing.

We also showed that *Sparc* is a previously underrecognized marker that distinguishes adaptive proliferation from constitutive proliferation in homeostasis (Table 1). SPARC, or osteonectin, is a secreted protein that has been studied for its role in corneal wound healing (75–79). Our scRNAseq data complement these previous studies by highlighting that *Sparc* is up-regulated specifically in proliferating cells of adaptive regeneration. We also show that SPARC protein is strongly expressed at the leading edge of wound corneal epithelium and that SPARC treatment accelerates scratch closure in human corneal epithelial cells, consistent with a previous study showing that treatment with exogenous SPARC accelerated corneal wound healing (78). We also identified SPARC target genes, several of which are known to be activated in corneal epithelial wound healing including FN1. Taken together, our data suggest that SPARC may be a key molecule coordinating the conserved ocular surface response to desiccative stress and injury. We also identified *Krt16* as a marker that distinguishes differentiated cells in the adaptive program from those in homeostasis (Table 1), consistent with a role for this keratin in wound healing that has been described in other epithelial tissues (80).

Finally, this scRNAseq transcriptional dissection of the corneal epithelium in homeostasis and DED also enabled key findings critically relevant to the long-standing search for LSC markers. We show that LSC markers that remain restricted to LSCs can be classified as stringent, in contrast to labile LSC markers that expand their expression dramatically in DED (Table 2). In our dataset, *Krt14, Lgals7,* and *Ifitm3* expanded expression to several DED-elicited cell types, consistent with previous work that has demonstrated that *Krt14* expression expands after corneal injury (65). On the other hand, stringent LSC markers like *Gpha2* among others appear to be faithfully restricted to LSCs even in injury. We also demonstrate that some LSC markers are semistringent and have nonspecific expression in either immune cells or DED-elicited LSC-like* cells (Table 2). This classification of LSC markers is of practical significance and may aid in the isolation of LSCs, especially which to use in homeostasis vs. disease contexts involving ocular surface injury. We thereby provide more granular and nuanced insight into the transcriptional hallmarks defining corneal epithelial stem cells in health and disease, which is critically important given the lack of consensus on a widely accepted LSC marker.

Overall, this study is a significant advance in our understanding of the function of a poorly characterized yet critically important ocular stem cell lineage. LSCs are crucial for maintaining visual function by renewing and regenerating a clear ocular surface under physiologic and pathologic conditions. We have resolved transcriptional signatures of corneal epithelial differentiation in health and disease, identified unique genes and gene networks that may be amenable to therapy, and created a framework for future studies of LSCs and other ocular surface stem cell compartments.

Materials and Methods

We generated mouse models of diabetes with streptozotocin, DED by excising lacrimal glands, and corneal epithelial injury using an AlgerBrush II. We performed scRNAseq using the 10× Genomics platform with analysis using the Seurat package (81). We validated scRNAseq data with immunostaining of mouse tissue along with RNA sequencing and scratch wound healing assay of a human corneal epithelial cell line. Experimental details are described in *SI Appendix, Materials and Methods*.

Data, Materials, and Software Availability. Genomic data have been deposited in Gene Expression Omnibus (GSE182419; GSE182477; GSE182583; GSE182582; GSE215149) (82–86).

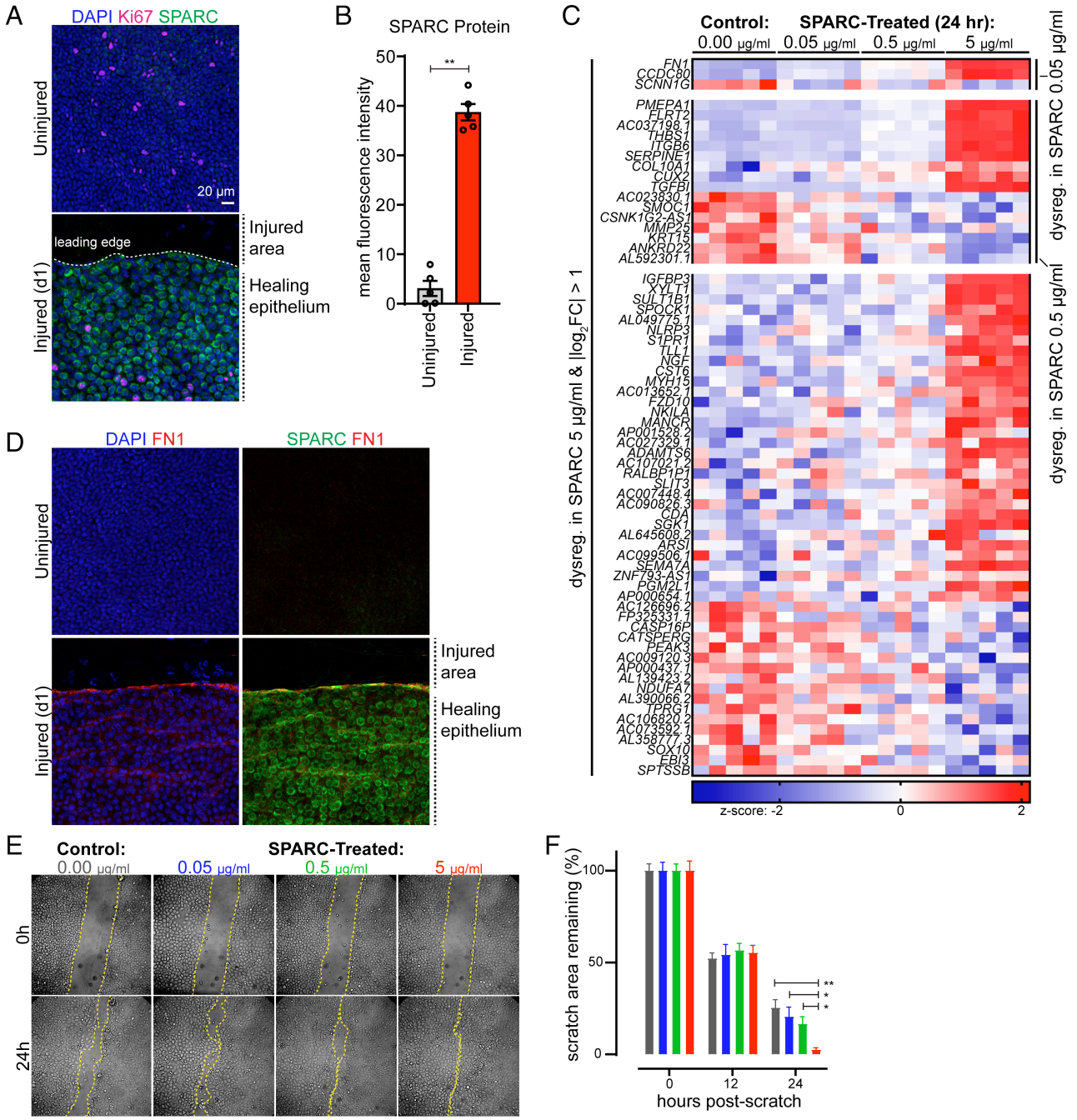

Fig. 6. Role of SPARC in corneal epithelial wound healing. (*A*) Immunostaining for SPARC and Ki67 at 1 d following mechanical debridement of the central corneal epithelium. These images are of flat-mounted corneas and are maximum projections of the entire corneal epithelium. (*B*) Quantification of mean SPARC fluorescence intensity. Bars indicate mean ± SEM, and each circle represents an individual eye. Statistical significance was assessed using the Mann–Whitney test. (*C*) Heat map showing target genes of SPARC in human corneal epithelial cells. (*D*) Immunostaining for SPARC and FN1 at 1 d following mechanical debridement of the central corneal epithelium. These images are of flat-mounted corneas and are maximum projections of the entire corneal epithelium. (Scale bar same as shown for Fig. 6*A*.) (*E*) Representative images of scratch assay performed with human corneal epithelial cells when treated with SPARC. Yellow dashed lines indicate the edge of the cell-free scratch area. (*F*) Quantification of the remaining cell-free area relative to each treatment group's initial average wound size. Each bar is colored corresponding to the labels in Fig. 7*E* and indicates the mean ± SEM calculated for n = 11 to 13 total scratches across three independent experiments. Statistical significance was assessed using the Brown–Forsythe ANOVA test for each time point (24-h omnibus *P* value < 0.01). For the 24-h time point, we performed a post hoc Dunnett's T3 multiple comparisons test for all pairwise comparisons. **P* < 0.05 and ***P* < 0.01.

ACKNOWLEDGMENTS. This work was supported by the NIH grants R01 EY019287 (R.S.A.), R00 EY027844 (B.S.C.), R01 EY024704 (Q.L.), and P30 EY02687 (Vision Core Grant); Jeffery T. Fort Innovation Fund (R.S.A.); Centene Corporation contract (P19-00559) for the Washington University-Centene ARCH Personalized Medicine Initiative; Siteman Research Fund; and an unrestricted grant from the Research to Prevent Blindness to the John F. Hardesty, MD Department of Ophthalmology and Visual Sciences at the Washington University School of Medicine in St. Louis. J.B.L. was supported by the NIH grant F30 DK130282 and the Washington University in St. Louis Medical Scientist Training Program (NIH grant T32 GM07200). We also thank Washington University's Genome Technology Access Center for help with scRNAseq studies, the Morphology & Imaging Core for assistance with paraffin sectioning and staining (Washington University Department of Ophthalmology & Visual Sciences), and Dr. Todd Margolis and Nicolas Ledru for helpful discussions.

1. N. Di Girolamo, Moving epithelia: Tracking the fate of mammalian limbal epithelial stem cells. *Prog. Retin. Eye Res.* **48**, 203–225 (2015).
2. H. F. Chew, Limbal stem cell disease: Treatment and advances in technology. *Saudi J. Ophthalmol.* **25**, 213–218 (2011).
3. A. Schermer, S. Galvin, T. T. Sun, Differentiation-related expression of a major 64K corneal keratin in vivo and in culture suggests limbal location of corneal epithelial stem cells. *J. Cell Biol.* **103**, 49–62 (1986).
4. R. A. Thoft, J. Friend, The X, Y, Z hypothesis of corneal epithelial maintenance. *Invest. Ophthalmol. Vis. Sci.* **24**, 1442–1443 (1983).
5. A. Altshuler *et al.*, Discrete limbal epithelial stem cell populations mediate corneal homeostasis and wound healing. *Cell Stem Cell* **28**, 1248–1261.e8 (2021).
6. O. Farrelly *et al.*, Two-photon live imaging of single corneal stem cells reveals compartmentalized organization of the limbal niche. *Cell Stem Cell* **28**, 1233–1247.e4 (2021).
7. R. Ishii, H. Yanagisawa, A. Sada, Defining compartmentalized stem cell populations with distinct cell division dynamics in the ocular surface epithelium. *Development* **147**, 197590 (2020).
8. R. Mittal, S. Patel, A. Galor, Alternative therapies for dry eye disease. *Curr. Opin. Ophthalmol.* **32**, 348–361 (2021).
9. J. Collin, A single cell atlas of human cornea that defines its development, limbal progenitor cells and their interactions with the immune cells. *Ocul. Surf.* **21**, 279–298 (2021), 10.1016/j.jtos.2021.03.010.
10. W. W. Kao *et al.*, Keratin 12-deficient mice have fragile corneal epithelia. *Invest. Ophthalmol. Vis. Sci.* **37**, 2572–2584 (1996).
11. C. Y. Liu *et al.*, Cornea-specific expression of K12 keratin during mouse development. *Curr. Eye Res.* **12**, 963–974 (1993).
12. C. Y. Liu *et al.*, Characterization and chromosomal localization of the cornea-specific murine keratin gene Krt1.12. *J. Biol. Chem.* **269**, 24627–24636 (1994).
13. T. T. Sun *et al.*, Monoclonal antibody studies of mammalian epithelial keratins: A review. *Ann. N. Y. Acad. Sci.* **455**, 307–329 (1985).
14. B. Zhao *et al.*, Targeted cornea limbal stem/progenitor cell transfection in an organ culture model. *Invest. Ophthalmol. Vis. Sci.* **49**, 3395–3401 (2008).
15. D. D. Miller, S. A. Hasan, N. L. Simmons, M. W. Stewart, Recurrent corneal erosion: A comprehensive review. *Clin. Ophthalmol.* **13**, 325–335 (2019).
16. P. Bargagna-Mohan *et al.*, Corneal nonmyelinating Schwann cells illuminated by single-cell transcriptomics and visualized by protein biomarkers. *J. Neurosci. Res.* **99**, 731–749 (2021).
17. P. M. Donisi, P. Rama, A. Fasolo, D. Ponzin, Analysis of limbal stem cell deficiency by corneal impression cytology. *Cornea* **22**, 533–538 (2003).
18. N. Kaplan *et al.*, Single-cell RNA transcriptome helps define the limbal/corneal epithelial stem/early transit amplifying cells and how autophagy affects this population. *Invest. Ophthalmol. Vis. Sci.* **60**, 3570–3583 (2019).
19. W. Macnair, M. Claassen, Psupertime: Supervised pseudotime inference for single cell RNA-seq data with sequential labels. bioRxiv [Preprint] (2019), https://doi.org/10.1101/622001. Accessed 14 July 2021.
20. H. Alam, L. Sehgal, S. T. Kundu, S. N. Dalal, M. M. Vaidya, Novel function of keratins 5 and 14 in proliferation and differentiation of stratified epithelial cells. *Mol. Biol. Cell* **22**, 4068–4078 (2011).
21. J.-M. Yang, S. M. Sim, H.-Y. Kim, G. T. Park, Expression of the homeobox gene, HOPX, is modulated by cell differentiation in human keratinocytes and is involved in the expression of differentiation markers. *Eur. J. Cell Biol.* **89**, 537–546 (2010).
22. S. Ren, T. Liu, C. Jia, X. Qi, Y. Wang, Physiological expression of lens α-, β-, and γ-crystallins in murine and human corneas. *Mol. Vis.* **16**, 2745–2752 (2010).
23. J. S. Swan, M. E. Arango, C. A. Carothers Carraway, K. L. Carraway, An ErbB2-Muc4 complex in rat ocular surface epithelia. *Curr. Eye Res.* **24**, 397–402 (2002).
24. T. F. Linsenmayer, C. X. Cai, J. M. Millholland, K. E. Beazley, J. M. Fitch, Nuclear ferritin in corneal epithelial cells: Tissue–specific nuclear transport and protection from UV–damage. *Prog. Retin. Eye Res.* **24**, 139–159 (2005).
25. S. Aibar *et al.*, SCENIC: Single-cell regulatory network inference and clustering. *Nat. Methods* **14**, 1083–1086 (2017).
26. B. Van de Sande *et al.*, A scalable SCENIC workflow for single-cell gene regulatory network analysis. *Nat. Protoc.* **15**, 2247–2276 (2020).
27. M. Aguilar-Medina *et al.*, SOX9 stem-cell factor: Clinical and functional relevance in cancer. *J. Oncol.* **2019**, 6754040 (2019).
28. V. Barbaro *et al.*, C/EBPδ regulates cell cycle and self-renewal of human limbal stem cells. *J. Cell Biol.* **177**, 1037–1049 (2007).
29. E. D. Iorio *et al.*, Isoforms of ΔNp63 and the migration of ocular limbal cells in human corneal regeneration. *Proc. Natl. Acad. Sci. U.S.A.* **102**, 9523–9528 (2005).
30. D. Hasegawa *et al.*, Epithelial Xbp1 is required for cellular proliferation and differentiation during mammary gland development. *Mol. Cell Biol.* **35**, 1543–1556 (2015).
31. S. Elias, E. J. Robertson, E. K. Bikoff, A. W. Mould, Blimp-1/PRDM1 is a critical regulator of type III interferon responses in mammary epithelial cells. *Sci Rep.* **8**, 237 (2018).
32. J. J. Miner *et al.*, HSV-1 and zika virus but not SARS-CoV-2 replicate in the human cornea and are restricted by corneal type III interferon. *Cell Rep.* **33**, 108339 (2020).
33. A. M. Verdoni, S. Ikeda, A. Ikeda, Serum response factor is essential for the proper development of skin epithelium. *Mamm. Genome* **21**, 64–76 (2010).
34. M. B. Schultz, D. A. Sinclair, When stem cells grow old: Phenotypes and mechanisms of stem cell aging. *Development* **143**, 3–14 (2016).
35. A. Richardson *et al.*, Keratin-14-Positive precursor cells spawn a population of migratory corneal epithelia that maintain tissue mass throughout life. *Stem Cell Rep.* **9**, 1081–1096 (2017).
36. P. Douvaras *et al.*, Rare corneal clones in mice suggest an age-related decrease of stem cell activity and support the limbal epithelial stem cell hypothesis. *Stem Cell Res.* **8**, 109–119 (2012).
37. M. Notara, A. J. Shortt, A. R. O'Callaghan, J. T. Daniels, The impact of age on the physical and cellular properties of the human limbal stem cell niche. *Age* **35**, 289–300 (2013).
38. O. Baylis, P. Rooney, F. Figueiredo, M. Lako, S. Ahmad, An investigation of donor and culture parameters which influence epithelial outgrowths from cultured human cadaveric limbal explants. *J. Cell Physiol.* **228**, 1025–1030 (2013).
39. N. Nieto-Nicolau, E. M. Martínez-Conesa, R. P. Casaroli-Marano, Limbal stem cells from aged donors are a suitable source for clinical application. *Stem Cells Int.* **2016**, 3032128 (2016).
40. A. V. Ljubimov, Diabetic complications in the cornea. *Vision Res.* **139**, 138–152 (2017).
41. K. C. Shih, K.S.-L. Lam, L. Tong, A systematic review on the impact of diabetes mellitus on the ocular surface. *Nutr. Diabetes* **7**, e251 (2017).
42. G. Bikbova, T. Oshitari, T. Baba, M. Bikbov, S. Yamamoto, Diabetic corneal neuropathy: Clinical perspectives. *Clin. Ophthalmol.* **12**, 981–987 (2018).
43. H. Sun, X. Mi, N. Gao, C. Yan, F.-S. Yu, Hyperglycemia-suppressed expression of serpine1 contributes to delayed epithelial wound healing in diabetic mouse corneas. *Invest. Ophthalmol. Vis. Sci.* **56**, 3383–3392 (2015).
44. I. S. Zagon, J. W. Sassani, J. A. Immonen, The opioid antagonist naltrexone reverses dry eye and enhances corneal wound healing in type II (db/db) mice. *FASEB J.* **25**, 1095.7 (2011).
45. J. He, T. L. Pham, A. Kakazu, H. E. P. Bazan, Recovery of corneal sensitivity and increase in nerve density and wound healing in diabetic mice after PEDF plus DHA treatment. *Diabetes* **66**, 2511–2520 (2017).
46. W. Li *et al.*, Leucine-rich α-2-glycoprotein-1 promotes diabetic corneal epithelial wound healing and nerve regeneration via regulation of matrix metalloproteinases. *Exp. Eye Res.* **196**, 108060 (2020).
47. X. Liu, H. Liu, X. Lu, J. Tombran-Tink, S. Zhao, PEDF attenuates ocular surface damage in diabetic mice model through its antioxidant properties. *Curr. Eye Res.* **46**, 302–308 (2021).
48. H. G. Matlock *et al.*, Pathogenic role of PPARα downregulation in corneal nerve degeneration and impaired corneal sensitivity in diabetes. *Diabetes* **69**, 1279–1291 (2020).
49. K. Ozaki, Y. Terayama, T. Matsuura, Extended duration of hyperglycemia result in human-like corneal nerve lesions in mice with alloxan- and Streptozotocin-induced type 1 diabetes. *Invest. Ophthalmol. Vis. Sci.* **59**, 5868–5875 (2018).
50. H. Sun *et al.*, Inhibition of soluble epoxide hydrolase 2 ameliorates diabetic keratopathy and impaired wound healing in mouse corneas. *Diabetes* **67**, 1162–1172 (2018).
51. X. Wang *et al.*, MANF Promotes diabetic corneal epithelial wound healing and nerve regeneration by attenuating hyperglycemia-induced endoplasmic reticulum stress. *Diabetes* **69**, 1264–1278 (2020).
52. C. Yan *et al.*, Targeting imbalance between IL-1β and IL-1 Receptor antagonist ameliorates delayed epithelium wound healing in diabetic mouse corneas. *Am. J. Pathol.* **186**, 1466–1480 (2016).
53. Z. Zhang *et al.*, Resolvin D1 promotes corneal epithelial wound healing and restoration of mechanical sensation in diabetic mice. *Mol. Vis.* **24**, 274–285 (2018).
54. K. Shinomiya, M. Ueta, S. Kinoshita, A new dry eye mouse model produced by exorbital and intraorbital lacrimal gland excision. *Sci. Rep.* **8**, 1483 (2018).
55. E. Ogawa *et al.*, Epidermal FABP (FABP5) regulates keratinocyte differentiation by 13(S)-HODE-mediated activation of the NF-κB signaling pathway. *J. Invest. Dermatol.* **131**, 604–612 (2011).
56. X. Zhang, M. Yin, L. Zhang, Keratin 6, 16 and 17–critical barrier alarmin molecules in skin wounds and psoriasis. *Cells* **8**, 807 (2019).
57. T. E. Ohara, M. Colonna, T. S. Stappenbeck, Adaptive differentiation promotes intestinal villus recovery. *Dev. Cell* **57**, 166–179.e6 (2022).
58. B. Shapiro, P. Tocci, G. Haase, N. Gavert, A. Ben-Ze'ev,, Clusterin, a gene enriched in intestinal stem cells, is required for L1-mediated colon cancer metastasis. *Oncotarget* **6**, 34389–34401 (2015).
59. L. Aj *et al.*, Molecular characteristics and spatial distribution of adult human corneal cell subtypes. *Sci. Rep.* **11**, 16323 (2021).
60. S. Dou *et al.*, Molecular identity of human limbal heterogeneity involved in corneal homeostasis and privilege. *Ocul Surf.* **21**, 206–220 (2021).
61. M. N. Nakatsu *et al.*, Preferential biological processes in the human limbus by differential gene profiling. *PLoS One* **8**, e61833 (2013).
62. D.-Q. Li *et al.*, Single-cell transcriptomics identifies limbal stem cell population and cell types mapping its differentiation trajectory in limbal basal epithelium of human cornea. *Ocul. Surf.* **20**, 20–32 (2021).
63. H. Peng, J. Wang, W. Yang, N. Kaplan, ID3/LRRK1 is a novel limbal epithelial stem cell regulatory axis. *Invest. Ophthalmol. Vis. Sci.* **61**, 2796 (2020).
64. Z. Su, J. Wang, Q. Lai, H. Zhao, L. Hou, KIT ligand produced by limbal niche cells under control of SOX10 maintains limbal epithelial stem cell survival by activating the KIT/AKT signalling pathway. *J. Cell Mol. Med.* **24**, 12020–12031 (2020).
65. M. Park *et al.*, Visualizing the contribution of keratin-14+ limbal epithelial precursors in corneal wound healing. *Stem Cell Rep.* **12**, 14–28 (2019).
66. K. Milde-Langosch, H. Kappes, S. Riethdorf, T. Löning, A.-M. Bamberger, FosB is highly expressed in normal mammary epithelia, but down-regulated in poorly differentiated breast carcinomas. *Breast Cancer Res. Treat.* **77**, 265–275 (2003).
67. J. T. Blanco-Mezquita, A. E. K. Hutcheon, M. A. Stepp, J. D. Zieske, αVβ6 integrin promotes corneal wound healing. *Invest. Ophthalmol. Vis. Sci.* **52**, 8505–8513 (2011).
68. J. Shen *et al.*, APR-246/PRIMA-1MET rescues epidermal differentiation in skin keratinocytes derived from EEC syndrome patients with p63 mutations. *Proc. Natl. Acad. Sci. U.S.A.* **110**, 2157–2162 (2013).
69. L. Latta *et al.*, Expression of retinoic acid signaling components ADH7 and ALDH1A1 is reduced in aniridia limbal epithelial cells and a siRNA primary cell based aniridia model. *Exp. Eye Res.* **179**, 8–17 (2019).
70. Y. Liu *et al.*, Pyruvate kinase M2 mediates glycolysis contributes to psoriasis by promoting keratinocyte proliferation. *Front. Pharmacol.* **12**, 765790 (2021).
71. R. L. Smathers, D. R. Petersen, The human fatty acid-binding protein family: Evolutionary divergences and functions. *Hum. Genomics* **5**, 170–191 (2011).
72. M. L. Fernandez, Z. Upton, G. K. Shooter, Uric acid and xanthine oxidoreductase in wound healing. *Curr. Rheumatol. Rep.* **16**, 396 (2013).
73. G. Xu, M. Redard, G. Gabbiani, P. Neuville, Cellular retinol-binding protein-1 is transiently expressed in granulation tissue fibroblasts and differentially expressed in fibroblasts cultured from different organs. *Am. J. Pathol.* **151**, 1741–1749 (1997).
74. C. Ngamkitidechakul, J. M. Burke, W. J. O'Brien, S. S. Twining, Maspin: Synthesis by human cornea and regulation of in vitro stromal cell adhesion to extracellular matrix. *Invest. Ophthalmol. Vis. Sci.* **42**, 3135–3141 (2001).
75. B. L. Berryhill, B. Kane, B. M. Stramer, M. E. Fini, J. R. Hassell, Increased SPARC accumulation during corneal repair. *Exp. Eye Res.* **77**, 85–92 (2003).
76. T. Latvala, P. Puolakkainen, M. Vesaluoma, T. Tervo, Distribution of SPARC protein (Osteonectin) in normal and wounded feline cornea. *Exp. Eye Res.* **63**, 579–584 (1996).
77. H. Mishima, T. Hibino, H. Hara, J. Murakami, T. Otori, SPARC from corneal epithelial cells modulates collagen contraction by keratocytes. *Invest. Ophthalmol. Vis. Sci.* **39**, 2547–2553 (1998).
78. L.-Y. Wang, Y.-T. Zhang, L.-Q. Du, X.-Y. Wu, J. Zhu, The Effect of SPARC on the proliferation and migration of limbal epithelial stem cells during the corneal epithelial wound healing. *Stem Cells Dev.* **30**, 301–308 (2021).
79. J. Zhu *et al.*, SPARC promotes self-renewal of limbal epithelial stem cells and ocular surface restoration through JNK and p38-MAPK signaling pathways. *Stem Cells* **38**, 134–145 (2020).
80. R. D. Paladini, K. Takahashi, N. S. Bravo, P. A. Coulombe, Onset of re-epithelialization after skin injury correlates with a reorganization of keratin filaments in wound edge keratinocytes: Defining a potential role for keratin 16. *J. Cell Biol.* **132**, 381–397 (1996).
81. Y. Hao *et al.*, Integrated analysis of multimodal single-cell data. *Cell* **184**, 3573–3587.e29 (2021).
82. J. B. Lin, R. S. Apte, scRNAseq of young vs. aged corneal epithelium. *Gene Expression Omnibus*. https://www.ncbi.nlm.nih.gov/geo/query/acc.cgi?acc=GSE182419. Deposited 19 August 2021.
83. J. B. Lin, R. S. Apte, scRNAseq of diabetic corneal epithelium. *Gene Expression Omnibus*. https://www.ncbi.nlm.nih.gov/geo/query/acc.cgi?acc=GSE182477. Deposited 19 August 2021.
84. J. B. Lin, R. S. Apte, scRNAseq of mouse corneal epithelium in homeostasis. *Gene Expression Omnibus*. https://www.ncbi.nlm.nih.gov/geo/query/acc.cgi?acc=GSE182583. Deposited 23 August 2021.
85. J. B. Lin, R. S. Apte, scRNAseq of corneal epithelium in dry eye disease. *Gene Expression Omnibus*. https://www.ncbi.nlm.nih.gov/geo/query/acc.cgi?acc=GSE182582. Deposited 23 August 2021.
86. J. B. Lin, R. S. Apte, RNA-seq of SPARC-treated human corneal epithelial cells. *Gene Expression Omnibus*. https://www.ncbi.nlm.nih.gov/geo/query/acc.cgi?acc=GSE215149. Deposited 10 October 2022.